Toxicol Res. (2022) 38:567–575
https://doi.org/10.1007/s43188-022-00139-z

eISSN 2234-2753
pISSN 1976-8257

ORIGINAL ARTICLE

Policosanol suppresses tumor progression in a gastric cancer xenograft model

Sunyi Lee[1] · Ga Seul Lee[2,3] · Jeong Hee Moon[3] · Joohee Jung[1,4]

Received: 18 April 2022 / Revised: 23 May 2022 / Accepted: 1 June 2022 / Published online: 5 July 2022

Abstract

Gastric cancer (GC) is the most common cancer worldwide and the third leading cause of cancer death, with the fifth highest incidence. The development of effective chemotherapeutic agents is needed to decrease GC mortality. Policosanol (PC) extracted from Cuban sugar cane wax is a healthy functional food ingredient that helps improve blood cholesterol levels and blood pressure. Its various physiological activities, such as antioxidant, anti-inflammatory, and anticancer activities, have been reported recently. Nevertheless, the therapeutic efficacy of PC in gastric xenograft models is unclear. We aimed to investigate the anticancer effect of PC on human GC SNU-16 cells and a xenograft mouse model. PC significantly inhibited GC cell viability and delayed tumor growth without toxicity in the SNU-16–derived xenograft model. Therefore, we investigated protein expression levels in tumor tissues; the expression levels of Ki-67, a proliferation marker, and cdc2 were decreased. In addition, we performed proteomic analysis and found thirteen differentially expressed proteins. Our results suggested that PC inhibited GC progression via cdc2 suppression and extracellular matrix protein regulation. Notably, our findings might contribute to the development of novel and effective therapeutic strategies for GC.

Keywords Gastric cancer · Policosanol · Xenograft mouse model · Healthy functional food · Extracellular matrix

Introduction

Gastric cancer (GC) incidence has been steadily declining; however, GC remains the most common and lethal neoplasm worldwide. According to global cancer statistics 2020, GC has the fifth highest incidence and is the fourth leading cause of cancer death [1]. GC treatments include endoscopic resection and chemotherapy [2]. Particularly, FOLFOX (oxaliplatin, 5-fluorouracil, and leucovorin calcium) and XELOX (oxaliplatin and capecitabine) are commonly used chemotherapy regimens [3], and other chemotherapeutic agents include paclitaxel, cisplatin, epirubicin, and etoposide [4]. Recently, personalized therapy, such as immunotherapy and targeted therapy, has been used to treat biomarker-defined GC subtypes [5]. Nevertheless, drug resistance and toxicity are obstacles to improving mortality. Therefore, the development of a novel anticancer agent is urgently needed for GC therapy.

Policosanol (PC) is a general term for active ingredients extracted from sugar cane wax. PC is a mixture of 1-tetracosanol, 1-hexacosanol, 1-heptacosanol, 1-octacosanol, 1-nonacosanol, 1-tricosanol, 1-dotriakosanol, and 1-tetratricosanol [6]. Particularly, PC extracted from Cuban sugar cane wax is a healthy functional food ingredient which helps improve blood cholesterol levels and regulate blood pressure. Additionally, PC exerts physiological effects, such as antioxidant, anti-inflammatory, and anticancer effects, prevents aging-related and cardiovascular diseases, and improves hypertension and hyperglycemia [7]. Moreover, 1-octacosanol, the main component of PC, exerts antinociceptive, anti-inflammatory, and anticancer effects [8–10]. However, because PC is a mixture of 1-octacosanol and other molecules, its mechanism is complex and remains to be elucidated. Thus, we aimed to investigate the mechanism and anticancer effect of PC in GC. To establish a GC xenograft model, we used

✉ Joohee Jung
joohee@duksung.ac.kr

1 Duksung Innovative Drug Center, Duksung Women's University, Seoul, Korea

2 College of Pharmacy, Chungbuk National University, Cheongju, Korea

3 Disease Target Structure Research Center, Korea Research Institute of Bioscience & Biotechnology, Daejeon, Korea

4 College of Pharmacy, Duksung Women's University, 33, Samyang-ro 144-gil, Dobong-gu, Seoul 01369, Korea

human gastric carcinoma SNU-16 cells, which were isolated from an Asian patient with GC before chemotherapy and which are commonly used in cancer research [11].

Materials and methods

PC

PC tablet (20 mg, Raydel®, Rainbow and Nature Pty. Ltd, Australia) was ground and added to 4 mL of 50% ethanol (Sigma-Aldrich; Merck KGaA, MA, USA). This suspension was ultrasonicated twice (Q700A-220, QSONICA, CT, USA) for 5 min at an amplitude of 50 (on/off, 10 s) [12–14].

Cell culture

SNU-16 cells (human GC cell line) were purchased from the Korean Cell Line Bank (no. 00016). The cells were incubated with Roswell Park Memorial Institute 1640 medium (GenDEPOT, TX, USA) containing 10% fetal bovine serum (GW Vitek, Seoul, Korea) and 1% penicillin/streptomycin (GenDEPOT) in a 5% CO_2 incubator at 37 °C.

Cell viability assay

SNU-16 cells ($0.5–1.0 \times 10^4$ cells/well) were seeded onto 96-well plates and incubated for 24 h. Serially diluted PC (finally diluted in 1% ethanol) was added to each well and then incubated for 24 and 48 h. Cell viability was measured using a cell counting kit (CCK)-8 assay (Dojindo Molecular Technologies, Inc., MD, USA). Briefly, 10 µL of CCK-8 reagent was added to each well and incubated at 37 °C for 3 h. Absorbance was measured at 450 nm using a microplate reader (Infinite M200 PRO, TECAN, Männedorf, Switzerland).

Animals

Balb/c-nude mice (BklNbt:BALB/c/nu/nu, female, 5 weeks old) were purchased from JA BIO (Gyeonggi, Korea). Animal experiments were performed according to a protocol approved by the Institutional Animal Care and Use Committee of Duksung Women's University (No. 2021-001-002) in compliance with the Guidelines for the Care and Use of Laboratory Animals. The mice were acclimatized for 1 week before the experiments and were maintained under optimal conditions at 22 ± 4 °C, 12 h light-dark cycle, and a relative humidity of 50–60%. Laboratory diet and drinking water were provided ad libitum.

Measurement of tumor growth and organ weight

SNU-16 cells (5×10^6 cells/100 µL) were injected subcutaneously into the right leg of 6-week-old female Balb/c-nude mice. Then, the mice were divided randomly into two groups: the PC-treated and control groups. From the day of transplantation, PC (100 mg/kg in 2% Tween 20) was administered orally 5 days a week. The control group was administered with the same amount of 2% Tween 20. Mouse body weight was measured thrice a week. Tumor length and width were measured using a caliper thrice a week. Thereafter, tumor volume was calculated from the Eq. 1 [15]:

$$\text{Tumor volume } (\text{mm}^3) = (\text{the longest length}) \times (\text{the shortest length})^2/2 \quad (1)$$

After the experiments, all experimental mice were sacrificed. The tumor, liver, kidney, and spleen were isolated and weighed.

Immunohistochemistry

Each tumor tissue was embedded in optimal cutting temperature compound (Leica Biosystems, Wetzlar, Germany) and frozen slowly at -20 °C. The frozen tissues were cut into 5 µm-thick slices using a cryostat (Leica Biosystems), and the sections were placed on a glass slide (MUTO Pure Chemicals Co., Ltd., Tokyo, Japan). The tumor tissue sections were treated with 3% H_2O_2 in methanol for 10 min and tap water for 10 min and then washed with phosphate-buffered saline (PBS). The sections were incubated with anti-Ki67 antibody (dilution, 1:200; Abcam, Cambridge, UK) at 4 °C overnight. After washing with PBS, the sections were treated with secondary goat anti-rabbit immunoglobulin (Ig) G (H + L)-horseradish peroxidase (HRP)–conjugated antibody (dilution, 1:100; BioRad Laboratories, Inc., CA, USA) at room temperature for 2 h. Antigen-antibody reactions were visualized using the VECTASTAIN Elite® ABC system (Vector Laboratories, CA, USA) and 3,3′-diaminobenzidine (Vector Laboratories), counterstained with hematoxylin, and mounted with limonene mounting medium (Abcam). The tissue sections were observed using microscopy (Leica).

Western blot analysis

Expression levels of antiproliferative proteins were determined using western blot analysis. Tumor tissues were lysed in radioimmunoprecipitation assay (RIPA) buffer (GenDEPOT) containing protease (P3100, GenDEPOT) and phosphatase (Roche, Basel, Switzerland) inhibitors. Protein concentration was measured using the Pierce™ bicinchoninic acid protein assay kit (Thermo Fisher Scientific, Inc., MA,

USA). Samples (25 µg of protein) were separated using 10–15% sodium dodecyl sulfate (SDS)-polyacrylamide gel electrophoresis using Mini-Protean Tetra cells and Power-PacTM Basic Power Supply (BioRad Laboratories, Inc.). Thereafter, the samples were transferred to polyvinylidene difluoride membranes at 0.15 A for 90 min using a Novex® semi-dry blotter (Invitrogen Co., CA, USA). The membranes were blocked with 5% blotting-grade blocker (BioRad Laboratories, Inc.) in Tris-buffered saline with 0.1% Tween 20 for 1 h at room temperature and then incubated with primary anti-extracellular signal-regulated kinase (ERK; Thermo Fisher Scientific, 1:1,000), anti-phosphorylated (p)ERK (Thermo Fisher Scientific, 1:1,000), anti-p-p53 (Santa Cruz Biotechnology, TX, USA, 1:500), anti-p53 (Merck Millipore, MA, USA, 1:1,000), anti-p21WAF1/Cip1 (Merck Millipore, 1:2,000), anti-cdc2 (Cell Signaling Technology, Inc., MA, USA, 1:1,000), and anti-glyceraldehyde-3-phosphate dehydrogenase (GAPDH; Enzo Life Sciences, Inc., NY, USA, 1:5,000) antibodies overnight at 4˚C. The next day, the membranes were incubated with the following secondary antibodies for 3 h at room temperature: goat anti-mouse IgG (H + L)-HRP–conjugated (BioRad Laboratories, Inc., 1:3,000) and goat anti-rabbit IgG (H + L)-HRP–conjugated (BioRad Laboratories, Inc., 1:3,000) antibodies. The proteins were detected using ChemiDoc (FluorChem E system, ProteinSimple, CA, USA) and an enhanced chemiluminescent solution and analyzed using AlphaView software for the FluorChem E system (version 3.4.0, Proteinsimple Inc.).

Protein extraction

Tumor tissues were homogenized in RIPA buffer (GenDEPOT) containing protease (GenDEPOT) and phosphatase (Roche) inhibitors on ice. After adding 10% SDS (finally diluted in 2% SDS) to the homogenized tissues, DNA and RNA were fragmented using ultrasonication (QSONICA) for 30 s at an amplitude of 50 (on/off, 3 s). Thereafter, homogenized tissues were heated at 95 °C for 10 min, and centrifuged at 25 °C and 13,000 × g for 10 min. The supernatants were used for proteomic analysis.

Digestion and isobaric labeling

Lysed proteins were digested using S-trap mini (ProtiFi, part no. C02-mini-80) following the manufacturer's protocol version 4.7 which includes the use of tris (2-carboxyethyl) phosphine and methyl methanethiosulfonate for reduction and alkylation. Thereafter, 10 µg of trypsin/Lys-C (Pierce, part no. A40009) was added to each sample and incubated for 1 h at 47℃. Eluted samples were dried using SpeedVac. Peptides were labeled with TMT 10-plex (Thermo Fisher Scientific, part no. 90,111) following the manufacturer's protocol. After 1 h of reaction, labeled peptides were mixed and desalted with Oasis HLB (Waters, part no. WAT186000383, 1 mL, 10 mg).

High-pH fraction

Peptide mixture were dried and dissolved with 5% acetonitrile (ACN)/10 mM ammonium bicarbonate. An Acquity UPLC Waters (Waters, Milford, MA) equipped with BEH C18 column (1.7 µm, 2.1 × 100 mm, part no. 186,002,352) and fraction collector (Gilson, FC203B) was used for fractionation. Buffers A and B contained 10 mM ammonium bicarbonate in distilled water and 90% ACN. The gradient was set from 5% B to 40% B in 79 min and from 40% B to 60% B in 16 min at a flow rate of 0.2 mL/min. Eluted solution was collected every 0.8 min. Every twenty-four elutions were combined to yield twenty-four sub-samples, such as e1, e25, e49, e73, e97-frac1, e2, e26, e50, e74, e98-frac2, etc. The samples were dried using SpeedVac.

Liquid chromatography with tandem mass spectrometry (LC/MS/MS) analysis

Ultimate 3000 RSLCnano coupled to an Orbitrap Exploris 240 mass spectrometer (MS, Thermo Fisher Scientific) was used for LC/MS/MS analysis. Each sample was dissolved in 0.1% formic acid/5% ACN, and peptides from 1 µg of protein were loaded onto the trap column (Acclaim PepMap 100, 75 µm × 2 cm, C18, 3 µm, PN 164,946). Peptides were separated using an analytical column (BEH300 C18, 75 µm × 25 cm, 1.7 µm, PN 186,003,815). The column temperature was set to 50℃. The mobile phases were 0.1% formic acid in water (buffer A) and 0.1% formic acid in ACN (buffer B). The following gradient was used at a flow rate of 300 nL/min: from 5% B to 7% B in 3 min, 7% B to 20% B in 73 min, 20% B to 28% B in 36 min, and 28% B to 60% B in 8 min. The survey scan settings were as follows: resolution, 120,000; max IT, auto; automatic gain control, 300%; mass range, 400–1600 Th. Selected precursor was fragmented by higher-energy collision dissociation and analyzed using Orbitrap MS. Other parameters for MS/MS scan were as follows: Top15 double play; resolution, 45,000; max IT, 80 ms; threshold 2E4; normalized collision energy, 36%; isolation width, 0.7; dynamic exclusion parameter exclude after n times, 1; exclusion duration time, 45 s; mass tolerance low/high, 10 ppm.

Data analysis

Raw data from LC/MS/MS were analyzed using Maxquant (version 2.0.3.0). Maxquant parameters were as follows: database UniProt Homo sapiens; enzyme, trypsin/P; variable modification, oxidation (M) and acetylation (protein N-term); fixed modification, methylthio (C); type, reporter

ion MS2 TMT10plex. Of various result files, proteinGroups.txt was used for further statistical analysis using Perseus (version 1.5.8.0). After reading the file, contaminant and reverse protein groups were filtered out. Protein groups were selected with a constraint that every experimental group contained at least two valid values. Missing values were replaced from a normal distribution. Thereafter, *p*-value was calculated for two of the three experimental groups. Significant proteins were selected based on fold change and *p*-value.

Statistical analysis

All data were analyzed using Student's t-test and analysis of variance (ANOVA) using GraphPad Prism 7 (GraphPad Software Inc., CA, USA). All data are expressed as the mean ± standard deviation (SD). $P < 0.05$ was considered statistically significant.

Results

PC inhibited GC cell viability

To investigate the anticancer effect of PC in GC SNU-16 cells, PC-induced cytotoxicity was assessed using CCK-8 assay (Fig. 1). PC inhibited SNU-16 cell viability in a dose-dependent manner. Notably, > 60 μg/mL PC significantly inhibited GC cell viability. Based on these results, we evaluated the therapeutic efficacy of PC in a xenograft mouse model.

PC suppressed tumor progression in an SNU-16–derived xenograft mouse model without toxicity

On the day of SNU-16 cell transplantation, PC (100 mg/kg) was orally administered. As shown in Fig. 2 A, the mice were treated 5 days a week for 5 weeks. In the control group,

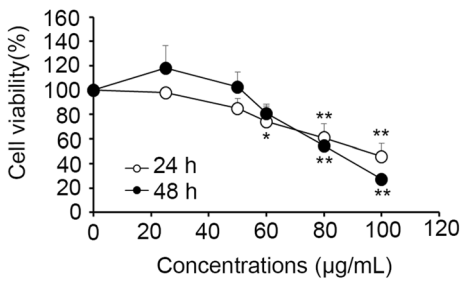

Fig. 1 PC inhibited SNU-16 cell viability. SNU-16 cells were treated with 25, 50, 60, 80, or 100 μg/mL PC for 24 and 48 h. The cell viability was evaluated using CCK-8 assay. All data are expressed as the mean ± SD of three independent experiments. *$p < 0.05$ and **$p < 0.001$ (one-way ANOVA with Dunnett's post hoc test)

two mice were excluded for ethical reasons due to poor conditions. Therefore, the number of mice in each group was different. Nevertheless, PC treatment significantly suppressed tumor growth; the tumor weights of PC-treated mice decreased, although not significantly, compared to those of control mice (Fig. 2B). To determine whether PC had any adverse effects, we measured and compared the body, liver, spleen, and kidney weights of the control and PC-treated groups. During the experimental period, we observed no significant differences in body weight gain between the control and PC-treated groups (Fig. 2C). In addition, no significant changes in liver, spleen, and kidney weights were observed between the control and PC-treated groups (Fig. 2D–F). These results indicated that PC delayed tumor growth without toxicity.

PC inhibited tumor proliferation by inhibiting cdc2

To elucidate the anticancer mechanism of PC, we used immunohistochemistry and western blotting to analyze tumor tissues. Particularly, we determined the expression levels of Ki-67, a proliferation marker. The PC-treated group showed a significant decrease in Ki-67 expression levels (Fig. 3A, B). Thus, PC inhibited tumor proliferation and suppressed tumor progression (Figs. 2A and 3A, B). Moreover, in the PC-treated group, the p-ERK1/2/ERK1/2 ratio decreased, which led to increased p53, p-p53, and p21 levels (not significant) and significantly decreased cdc2 levels (Fig. 3C, D). These results suggested that PC decreased the p-ERK1/2/ERK1/2 ratio and then induced p53 and p21, tumor suppressors. Furthermore, cdc2 levels decreased as p21 levels increased.

PC induced changes in the extracellular matrix (ECM) of SNU-16–derived tumor tissues

As shown in Fig. 3, PC inhibited GC cell proliferation. In addition, we performed proteomic analysis to investigate the role of PC in tumor progression. The differences in protein expression levels between the control and PC-treated groups were considered significant at fold change > 1.5 and $p < 0.05$ and are shown in Fig. 4; red dots indicate the proteins whose expression levels showed significant differences. As shown in Table 1, thirteen proteins were differentially expressed. The only upregulated proteins in the PC-treated group were elastin microfibril interfacer 1 (EMILIN-1), cytochrome c oxidase assembly factor COX19 (COX19), NEDD1 gamma-tubulin ring complex targeting factor (NEDD1), tenascin C (TNC), biglycan (BGN), arginase-1 (ARG1), dermatopontin (DPT), collagen type I alpha 1 chain (COL1A1),

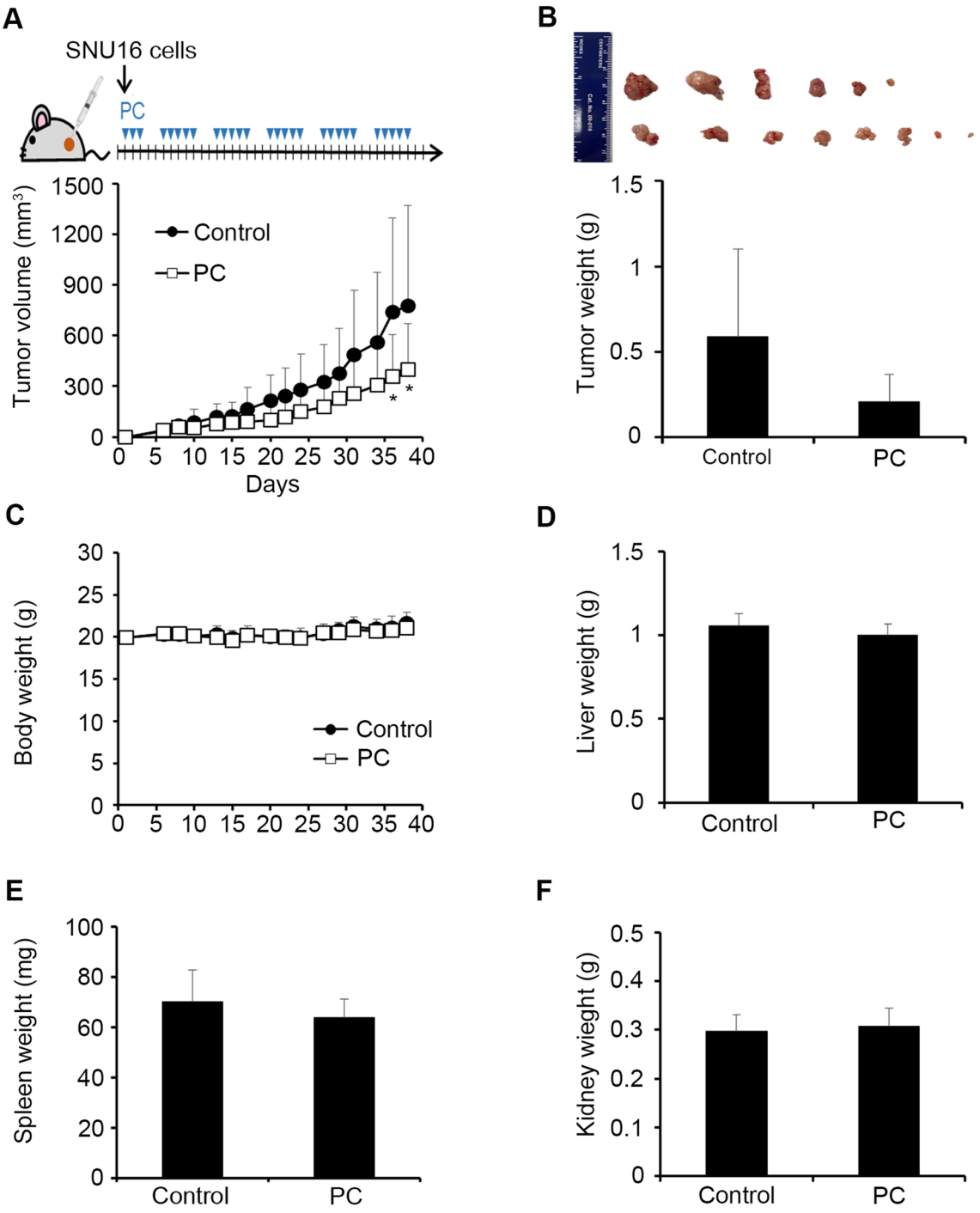

Fig. 2 PC delayed tumor growth in an SNU-16–derived xenograft mouse model without toxicity. **a** PC treatment schedule. Tumor volumes were calculated from the Eq. 1. **b** Comparison of tumor weights between the control and PC-treated groups. Isolated tumor tissues after the last measurement of tumor volume are shown. **c** Mouse body weight. Liver **d**, spleen **e**, and kidney **f** weights. Data are expressed as the mean ± SD (control group, n = 6; PC-treated group, n = 8). *$p < 0.05$ (two-way ANOVA with Sidak's post hoc test)

collagen type II alpha 2 chain (COL1A2), collagen type V alpha 1 chain (COL5A1), brain abundant membrane attached signal protein 1 (BASP1), collagen type IV alpha 2 chain (COL4A2), and microfibrillar-associated protein 5 (MFAP5). These results suggested that most differentially expressed proteins were ECM proteins and that PC treatment suppressed tumor growth in the SNU-16–derived xenograft mouse model.

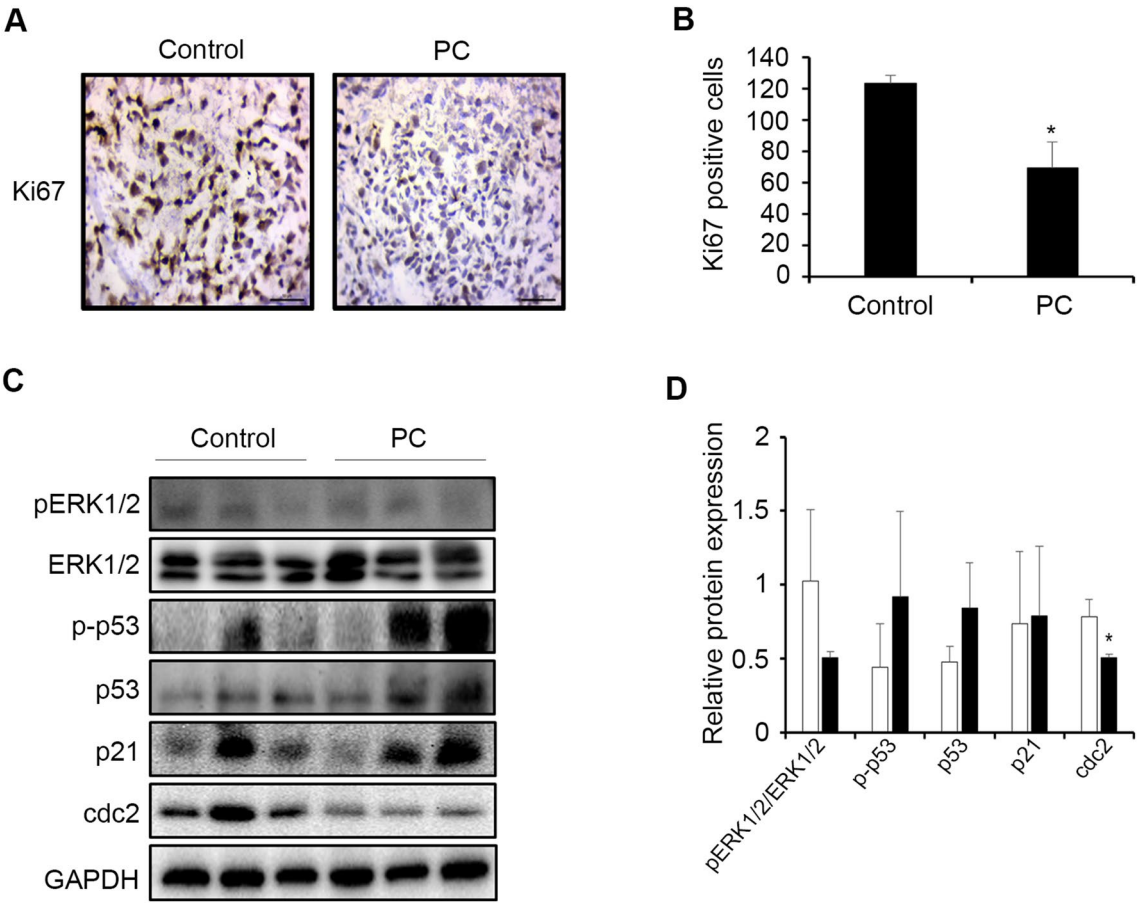

Fig. 3 PC activated the antiproliferative signaling pathway. **a** Ki-67 expression levels in tumor tissues. Brown dots indicate Ki-67-expressing cells. Scale bar, 50 μm (magnification, × 40). **b** Comparison of Ki-67 levels between the control and PC-treated groups. Data are expressed as the mean ± SD (n = 3/group). *$p < 0.01$ (Student's *t*-test). **c** The expression levels of pERK1/2, ERK1/2, p-p53, p53, p21, and cdc2 in tumor tissues. **d** Relative protein expression levels based on the values in **c**. The values indicate the ratio of protein to GAPDH levels. Data are expressed as the mean ± SD (n = 3/group). *$p < 0.05$ (Student's *t*-test)

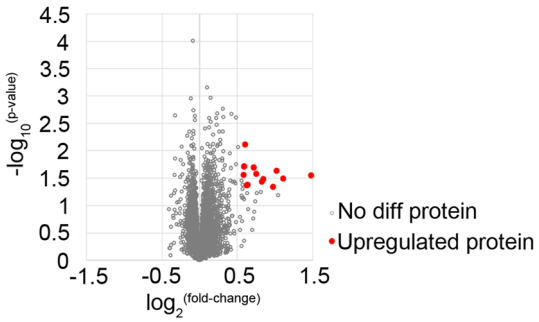

Fig. 4 Volcano plot of proteins. Visualization of differentially expressed proteins with volcano plot. Data show the relationship between large magnitude fold-changes ($\log_2$(fold change), X-axis) and high statistical significance ($-\log_{10}$(p − value), Y-axis). Red dots indicate significantly upregulated proteins

Table 1 List of the differentially expressed proteins

Protein name	Fold-change[a]	*p* value
EMILIN-1	1.5192	0.0078
COX19	1.5042	0.0193
NEDD1	1.6473	0.0204
TNC	2.0310	0.0231
BGN	1.6823	0.0263
ARG1	1.5033	0.0277
DPT	2.7839	0.0282
COL1A1	2.1623	0.0323
COL1A2	1.7972	0.0327
COL5A1	1.7774	0.0364
BASP1	1.5540	0.0418
COL4A2	1.5464	0.0427
MFAP5	1.9621	0.0456

[a]Ratio of the mean expression value. (Control group vs. PC-treated group)

Discussion

PC is a healthy functional food ingredient that helps improve cholesterol levels and blood pressure. Moreover, PC has various physiological activities in different cell lines [16]. In this study, PC showed therapeutic efficacy in a GC xenograft mouse model by inhibiting cell proliferation. In addition, we found several ECM proteins that were differentially expressed following PC treatment. Notably, tumor growth in PC-treated mice was significantly delayed compared with that in control mice (Fig. 2A). Aleman et al. reported that PC showed no carcinogenicity in 18-month-long chronic toxicity tests [17]. Our results also indicated that PC treatment did not affect the body and organ weights of xenograft mice (Fig. 2C–F). Several previous studies have demonstrated that PC conditionally modulates the AMPK, MAPK, and PI3K/Akt signaling pathways [18–20]. To elucidate the therapeutic efficacy of PC in the SNU-16–derived xenograft mouse model, we investigated the PC-regulated signaling pathway in tumor tissues. Moreover, we investigated the mechanism of PC, which is complex and remains unclear because PC contains numerous molecules. Particularly, only the octacosanol mechanism is well known. Wang et al. reported that octacosanol, a component of PC, significantly inhibits the mitochondrial permeability transition pore-induced phosphorylation of c-Jun N-terminal kinase and p38MAPK but not of ERK1/2 in mice [21]. Furthermore, Guo et al. reported that octacosanol attenuates intestinal inflammation in mice via MAPK signaling [10]. Notably, our results indicated that PC decreased the p-ERK1/2/ERK1/2 ratio and activated p53 and p21, thus downregulating cdc2 expression (Fig. 3C, D). Moreover, the PC-regulated signaling pathway induced anti-proliferation of SNU-16 gastric tumor cells. A similar signaling pathway was reported in GC AGS cells treated with tanshinone IIA, which induces G2/M phase arrest [22]. Intriguingly, cdc2 knockdown inhibits the proliferation and enhances the apoptosis of glioblastoma cells [23]. The decrease in Ki-67–expressing cells in the PC-treated group indicated cell anti-proliferation (Fig. 3A, B). These results suggested that PC showed therapeutic efficacy in GC by inhibiting cdc2.

In this study, we simultaneously administered PC and injected SNU-16 cells into the mice. To investigate whether PC was also associated with tumor progression, we further performed proteomic analysis of tumor tissues. Noteworthy, thirteen proteins were upregulated in the PC-treated group (Table 1), including eight ECM proteins, three cytosolic enzymes, a membrane-bound protein, and a mitosis-related protein. Various studies have demonstrated the relationship between these proteins and cancer progression. However, their role has not been reported or elucidated yet. The ECM plays a role in cancer microenvironment regulation and influences cancer progression [24]. Various ECM molecules display opposing functions in a time-dependent or tissue-specific manner [25]. The proteomic analysis also revealed that PC upregulated several ECM molecules, including EMILIN-1. EMILIN-1 is less expressed in breast cancer than in normal tissue [26], and EMILIN-1–negative microenvironment aggravates cancer progression [27]. Particularly, melanoma progression and metastasis are favored by EMILIN-1 inactivation by proteolysis and its secretion via small extracellular vesicles [28]. Additionally, EMILIN-1 exerts an anticancer effect in GC by upregulating tetraspanin 9 expression [29]. Our results indicated that PC increased EMILIN-1 levels and inhibited GC tumor growth. Thus, EMILIN-1 could be a biomarker for targeted chemotherapy of GC. Unfortunately, among the factors found in the proteomic analysis, several collagen alpha chain subtypes and TNC, BGN, and MFAP5 are aggressive factors in various cancers. Notably, high COL1A1 expression levels are observed in breast [30], colorectal [31], lung [32], and gastric cancers [33]. In the present study, COL4A2 and COL5A1, which induce cell proliferation, migration, invasion, and metastasis, were also upregulated. The COL1A2 level in PC-treated tumor tissues was also high. This COL1A2 is reported to inhibit colorectal cancer progression [34]. TNC [35], BGN [36], and MFAP5 [37] are overexpressed in various cancers and are associated with cancer aggressiveness. Also, several proteins related to inhibiting cancer progression are found in PC-treated tumor tissues. DPT expression levels are lower in endometrial cancer than in normal tissue [38]. Furthermore, NEDD1 [39] and ARG1 [40] are promising targets for inhibiting cancer progression. High BASP1 expression levels are associated with high overall survival in patients with pancreatic cancer [41]. Our results demonstrated that these proteins were upregulated by PC treatment in the SNU-16–derived xenograft mouse model. These proteins warrant further investigation to elucidate their role in GC progression.

Notably, we revealed that PC inhibited cancer proliferation via cdc2 and upregulated ECM molecules in the SNU-16–derived xenograft mouse model, which suggested that PC could be used as an adjuvant therapy in GC.

Funding Tis research was funded by Ministry of Education, Grant no [2021R1A6A3A01086368], NRF by Korea, Grant no [2021R1A2C200453511] and the Priority Research Centers Program through the NRF, Grant no [2016R1A6A1A03007648].

Declarations

Conflict of interest The authors have not disclosed any competing interests.

References

1. Sung H, Ferlay J, Siegel RL, Laversanne M, Soerjomataram I, Jemal A, Bray F (2021) Global Cancer Statistics 2020: GLOBOCAN estimates of incidence and mortality worldwide for 36 cancers in 185 countries. CA Cancer J Clin 71:209–249. https://doi.org/10.3322/caac.21660
2. Petrillo A, Smyth EC (2020) Biomarkers for precision treatment in gastric cancer. Visc Med 36:364–372. https://doi.org/10.1159/000510489
3. Xu HB, Huang F, Su R, Shen FM, Lv QZ (2015) Capecitabine plus oxaliplatin (XELOX) compared with 5-fluorouracil/leucovorin plus oxaliplatin (FOLFOXs) in advanced gastric cancer: meta-analysis of randomized controlled trials. Eur J Clin Pharmacol 71:589–601. https://doi.org/10.1007/s00228-015-1828-9
4. Sudo K, Yamada Y (2015) Advancing pharmacological treatment options for advanced gastric cancer. Expert Opin Pharmacother 16:2293–2305. https://doi.org/10.1517/14656566.2015.1080238
5. Joshi SS, Badgwell BD (2021) Current treatment and recent progress in gastric cancer. CA Cancer J Clin 71:264–279. https://doi.org/10.3322/caac.21657
6. Shen J, Luo F, Lin Q (2019) Policosanol: Extraction and biological functions. J Funct Food 57:351–360. https://doi.org/10.1016/j.jff.2019.04.024
7. Jang YS, Kim DE, Han E, Jung J (2019) Physiological activities of policosanol extracted from sugarcane wax. Nat Prod Sci 25:293–297. https://doi.org/10.20307/nps.2019.25.4.293
8. de Oliveira AM, Conserva LM, de Souza Ferro JN, de Almeida Brito F, Lyra Lemos RP, Barreto E (2012) Antinociceptive and anti-inflammatory effects of octacosanol from the leaves of *Sabicea grisea* var. grisea in mice. Int J Mol Sci 13:1598–1611. https://doi.org/10.3390/ijms13021598
9. Thippeswamy G, Sheela ML, Salimath BP (2008) Octacosanol isolated from *Tinospora cordifolia* downregulates VEGF gene expression by inhibiting nuclear translocation of NF-κB and its DNA binding activity. Eur J Pharmacol 588:141–150. https://doi.org/10.1016/j.ejphar.2008.04.027
10. Guo T, Lin Q, Li X, Nie Y, Wang L, Shi L, Xu W, Hu T, Guo T, Luo F (2017) Octacosanol attenuates inflammation in both RAW264.7 macrophages and a mouse model of colitis. J Agric Food Chem 65:3647–3658. https://doi.org/10.1021/acs.jafc.6b05465
11. Park JG, Frucht H, LaRocca RV, Bliss DP Jr, Kurita Y, Chen TR, Henslee JG, Trepel JB, Jensen RT, Johnson BE et al (1990) Characteristics of cell lines established from human gastric carcinoma. Cancer Res 50:2773–2780. https://pubmed.ncbi.nlm.nih.gov/2158397
12. Banerjee S, Ghoshal S, Porter TD (2011) Activation of AMP-kinase by policosanol requires peroxisomal metabolism. Lipids 46:311–321. https://doi.org/10.1007/s11745-011-3540-6
13. Ishaka A, Umar Imam M, Mahamud R, Zuki AB, Maznah I (2014) Characterization of rice bran wax policosanol and its nanoemulsion formulation. Int J Nanomed 9:2261–2269. https://doi.org/10.2147/IJN.S56999
14. Kim JY, Lee JH, Jeong DY, Jang DK, Seo TR, Lim ST (2015) Preparation and characterization of aqueous dispersions of dextrin and policosanol composites. Carbohydr Polym 121:140–146. https://doi.org/10.1016/j.carbpol.2014.12.050
15. Oh S, Kwon HJ, Jung J (2022) Estrogen exposure causes the progressive growth of SK-Hep1-derived tumor in ovariectomized mice. Toxicol Res 38:1–7. https://doi.org/10.1007/s43188-021-00100-6
16. Singh DK, Li L, Porter TD (2006) Policosanol inhibits cholesterol synthesis in hepatoma cells by activation of AMP-kinase. J Pharmacol Exp Ther 318:1020–1026. https://doi.org/10.1124/jpet.106.107144
17. Aleman CL, Puig MN, Elias EC, Ortega CH, Guerra IR, Ferreiro RM, Briñis F (1995) Carcinogenicity of policosanol in mice: an 18-month study. Food Chem Toxicol 33:573–578. https://doi.org/10.1016/0278-6915(95)00026-x
18. Lee JH, Jia Y, Thach TT, Han Y, Kim B, Wu C, Kim Y, Seo WD, Lee SJ (2017) Hexacosanol reduces plasma and hepatic cholesterol by activation of AMP-activated protein kinase and suppression of sterol regulatory element-binding protein-2 in HepG2 and C57BL/6J mice. Nutr Res 43:89–99. https://doi.org/10.1016/j.nutres.2017.05.013
19. Liu YW, Zuo PY, Zha XN, Chen XL, Zhang R, He XX, Liu CY (2015) Octacosanol enhances the proliferation and migration of human umbilical vein endothelial cells via activation of the PI3K/Akt and MAPK/Erk pathways. Lipids 50:241–251. https://doi.org/10.1007/s11745-015-3991-2
20. Varady KA, Wang Y, Jones PJ (2003) Role of policosanols in the prevention and treatment of cardiovascular disease. Nutr Rev 61:376–383. https://doi.org/10.1301/nr.2003.nov.376-383
21. Wang T, Liu Y, Yang N, Ji C, Chan P, Zuo P (2012) Anti-parkinsonian effects of octacosanol in 1-methyl-4-phenyl-1,2,3,6 tetrahydropyridine-treated mice. Neural Regen Res 7:1080–1087. https://doi.org/10.3969/j.issn.1673-5374.2012.14.006
22. Su CC (2014) Tanshinone IIA inhibits gastric carcinoma AGS cells through increasing p-p38, p-JNK and p53 but reducing p-ERK, CDC2 and cyclin B1 expression. Anticancer Res 34:7097–7110. https://pubmed.ncbi.nlm.nih.gov/25503137
23. Zhou B, Bu G, Zhou Y, Zhao Y, Li W, Li M (2015) Knockdown of CDC2 expression inhibits proliferation, enhances apoptosis, and increases chemosensitivity to temozolomide in glioblastoma cells. Med Oncol 32:378. https://doi.org/10.1007/s12032-014-0378-9
24. Henke E, Nandigama R, Ergun S (2019) Extracellular matrix in the tumor microenvironment and its impact on cancer therapy. Front Mol Biosci 6:160. https://doi.org/10.3389/fmolb.2019.00160
25. Nallanthighal S, Heiserman JP, Cheon DJ (2019) The role of the extracellular matrix in cancer stemness. Front Cell Dev Biol 7:86. https://doi.org/10.3389/fcell.2019.00086
26. Rabajdova M, Urban P, Spakova I, Saksun L, Dudic R, Ostro A, Caprnda M, Kruzliak P, Adamek M, Marekova M (2016) The crucial role of emilin 1 gene expression during progression of tumor growth. J Cancer Res Clin Oncol 142:2397–2402. https://doi.org/10.1007/s00432-016-2226-0
27. Danussi C, Petrucco A, Wassermann B, Modica TM, Pivetta E, Del Bel Belluz L, Colombatti A, Spessotto P (2012) An EMILIN1-negative microenvironment promotes tumor cell proliferation and lymph node invasion. Cancer Prev Res (Phila) 5:1131–1143. https://doi.org/10.1158/1940-6207.CAPR-12-0076-T
28. Amor López A, Mazariegos MS, Capuano A, Ximénez-Embún P, Hergueta-Redondo M, Recio J, Muñoz E, Al-Shahrour F, Muñoz J, Megías D, Doliana R, Spessotto P, Peinado H (2021) Inactivation of EMILIN-1 by proteolysis and secretion in small extracellular vesicles favors melanoma progression and metastasis. Int J Mol Sci 22:7406. https://doi.org/10.3390/ijms22147406
29. Qi Y, Lv J, Liu S, Sun L, Wang Y, Li H, Qi W, Qiu W (2019) TSPAN9 and EMILIN1 synergistically inhibit the migration and

invasion of gastric cancer cells by increasing TSPAN9 expression. BMC Cancer 19:630. https://doi.org/10.1186/s12885-019-5810-2
30. Liu J, Shen JX, Wu HT, Li XL, Wen XF, Du CW, Zhang GJ (2018) Collagen 1A1 (COL1A1) promotes metastasis of breast cancer and is a potential therapeutic target. Discov Med 25:211–223. https://pubmed.ncbi.nlm.nih.gov/25503137
31. Zhang Z, Wang Y, Zhang J, Zhong J, Yang R (2018) COL1A1 promotes metastasis in colorectal cancer by regulating the WNT/PCP pathway. Mol Med Rep 17:5037–5042. https://doi.org/10.3892/mmr.2018.8533
32. Hou L, Lin T, Wang Y, Liu B, Wang M (2021) Collagen type 1 alpha 1 chain is a novel predictive biomarker of poor progression-free survival and chemoresistance in metastatic lung cancer. J Cancer 12:5723–5731. https://doi.org/10.7150/jca.59723
33. Dong XZ, Zhao ZR, Hu Y, Lu YP, Liu P, Zhang L (2020) LncRNA COL1A1-014 is involved in the progression of gastric cancer via regulating CXCL12-CXCR4 axis. Gastric Cancer 23:260–272. https://doi.org/10.1007/s10120-019-01011-0
34. Yu Y, Liu D, Liu Z, Li S, Ge Y, Sun W, Liu B (2018) The inhibitory effects of COL1A2 on colorectal cancer cell proliferation, migration, and invasion. J Cancer 9:2953–2962. https://doi.org/10.7150/jca.25542
35. Yoshida T, Akatsuka T, Imanaka-Yoshida K (2015) Tenascin-C and integrins in cancer. Cell Adh Migr 9:96–104. https://doi.org/10.1080/19336918.2015.1008332
36. Zhao SF, Yin XJ, Zhao WJ, Liu LC, Wang ZP (2020) Biglycan as a potential diagnostic and prognostic biomarker in multiple human cancers. Oncol Lett 19:1673–1682. https://doi.org/10.3892/ol.2020.11266
37. Yeung TL, Leung CS, Yip KP, Sheng J, Vien L, Bover LC, Birrer MJ, Wong STC, Mok SC (2019) Anticancer Immunotherapy by MFAP5 blockade inhibits fibrosis and enhances chemosensitivity in ovarian and pancreatic cancer. Clin Cancer Res 25:6417–6428. https://doi.org/10.1158/1078-0432.CCR-19-0187
38. Huang H, Hao Z, Long L, Yin Z, Wu C, Zhou X, Zhang B (2021) Dermatopontin as a potential pathogenic factor in endometrial cancer. Oncol Lett 21:408. https://doi.org/10.3892/ol.2021.12669
39. Tillement V, Haren L, Roullet N, Etievant C, Merdes A (2009) The centrosome protein NEDD1 as a potential pharmacological target to induce cell cycle arrest. Mol Cancer 8:10. https://doi.org/10.1186/1476-4598-8-10
40. Rodriguez PC, Quiceno DG, Zabaleta J, Ortiz B, Zea AH, Piazuelo MB, Delgado A, Correa P, Brayer J, Sotomayor EM, Antonia S, Ochoa JB, Ochoa AC (2004) Arginase I production in the tumor microenvironment by mature myeloid cells inhibits T-cell receptor expression and antigen-specific T-cell responses. Cancer Res 64:5839–5849. https://doi.org/10.1158/0008-5472.CAN-04-0465
41. Zhou Q, Andersson R, Hu D, Bauden M, Kristl T, Sasor A, Pawłowski K, Pla I, Hilmersson KS, Zhou M, Lu F, Marko-Varga G, Ansari D (2019) Quantitative proteomics identifies brain acid soluble protein 1 (BASP1) as a prognostic biomarker candidate in pancreatic cancer tissue. EBioMedicine 43:282–294. https://doi.org/10.1016/j.ebiom.2019.04.008